Photoinduced Oxidative Addition of a Distal Aromatic C–H Bond of a Benzyl Group. Isolation and Characterization of $(\eta^5\text{-}C_5R_4CH_2\overline{C_6H_4})Fe(CO)_2$ from Irradiation of $(\eta^5\text{-}C_5R_4CH_2C_6H_5)Fe(CO)_2Me$

Josephine Paw Blaha, John C. Dewan, and Mark S. Wrighton*

Department of Chemistry, Massachusetts Institute of Technology, Cambridge, Massachusetts 02139

Received August 29, 1985

Near-UV irradiation of $(\eta^5\text{-}C_5R_4CH_2C_6H_5)Fe(CO)_2Me$ (R = H, Me) yields both loss of CO and Me radicals, although loss of CO dominates the excited-state chemistry. In the absence of 2e donor ligands, the CO loss product undergoes oxidative addition of the ortho C–H bond of the coordinated benzyl group to yield the cyclometalated products $(\eta^5\text{-}C_5R_4CH_2\overline{C_6H_4})Fe(CO)_2$. For R = Me, the quantum efficiency for CO loss to yield the oxidative addition product (ϕ_{366nm} = 0.40) is nearly the same as the quantum efficiency for CO loss in the presence of PPh_3 to yield the substitution product $(\eta^5\text{-}C_5Me_4CH_2C_6H_5)Fe(CO)(PPh_3)Me$ (ϕ_{366nm} = 0.46). For R = H, however, the quantum efficiency for formation of the oxidative addition product ($\phi_{366nm} \approx 0.05$) is much smaller than the quantum efficiency for CO loss in the presence of PPh_3 to yield the substitution product $(\eta^5\text{-}C_5H_4CH_2C_6H_5)Fe(CO)(PPh_3)Me$ (ϕ_{366nm} = 0.70). Irradiation of the hydride $(\eta^5\text{-}C_5Me_4CH_2C_6H_5)Fe(CO)_2H$ also gives the oxidative addition product but in much smaller yield. The oxidative addition can be reversed by photoreaction of the cyclometalated species under H_2 or D_2; thus the photoreaction of $(\eta^5\text{-}C_5Me_4CH_2\overline{C_6H_4})Fe(CO)_2$ with D_2 yields $(\eta^5\text{-}C_5Me_4CH_2C_6H_4D)Fe(CO)_2D$. The cyclometalated products were isolated and characterized. The crystal structure of $(\eta^5\text{-}C_5Me_4CH_2\overline{C_6H_4})Fe(CO)_2$ was determined to unambiguously establish its structure; crystal data are a = 9.230 (2) Å, b = 15.321 (4) Å, c = 11.531 (2) Å, β = 109.76 (1)°, V = 1534.6 Å^3, space group = $P2_1/n$, final R_1 = 0.050, and R_2 = 0.073.

In this paper we wish to report a new finding concerning the photochemistry of benzyl-substituted cyclopentadienyl iron dicarbonyl methyl: the photoinduced oxidative addition of an aromatic C–H bond of a distal benzyl group to the Fe center. When $(\eta^5\text{-}C_5R_4Bz)Fe(CO)_2Me$ (R = H, Me; Bz = $CH_2C_6H_5$) is irradiated with near-UV light, the cyclometalated species $(\eta^5\text{-}C_5R_4CH_2\overline{C_6H_4})Fe(CO)_2$ are formed via dissociative loss of CO as the primary photoreaction.

Research in our laboratory[1,2] and elsewhere[3-5] has established that photoexcitation of $(\eta^5\text{-}C_5R_5)Fe(CO)_2R'$ (R = H, Me; R' = Me, Bz) leads to two principal modes of decay. Dissociative loss of CO occurs with great efficiency ($\phi_{366nm} \approx 0.5$–0.7) to yield 16e unsaturated species which can react with 2e donor ligands L such as PPh_3 to yield the substitution products $(\eta^5\text{-}C_5R_5)Fe(CO)(L)(R')$ (eq 1).

$$(\eta^5\text{-}C_5R_5)Fe(CO)_2R' + L \xrightarrow[298\ K]{h\nu} (\eta^5\text{-}C_5R_5)Fe(CO)(L)(R') + CO \quad (1)$$

A less efficient ($\phi_{366nm} < 0.1$), but nonetheless important, decay path is homolytic cleavage of the Fe–C bond to yield $(\eta^5\text{-}C_5R_5)Fe(CO)_2$ and R radicals. The photogenerated radicals can simply couple, or the $(C_5R_5)Fe(CO)_2$ radical can first react with 2e donor ligands such as CO or PPh_3 and then couple with R' to form the diene iron tricarbonyls $(\eta^4\text{-}C_5R_5R')Fe(CO)_3$ or a substitution derivative (eq 2).

$$(\eta^5\text{-}C_5R_5)Fe(CO)_2\cdot + R'\cdot \xrightarrow[h\nu,\ L]{298\ K} (\eta^4\text{-}C_5R_5R')Fe(CO)_2L \quad (2)$$

$$L = CO,\ PPh_3$$

Our present results show a new mode of reactivity for the photogenerated 16e unsaturated fragment resulting from dissociative loss of CO. This 16e species can oxidatively add a distal aromatic C–H bond of a benzyl group to yield products $(\eta^5\text{-}C_5R_4CH_2\overline{C_6H_4})Fe(CO)_2$ that result from the reductive elimination of CH_4 (eq 3–6).

$$(\eta^5\text{-}C_5R_4Bz)Fe(CO)_2Me \xrightarrow{h\nu} (\eta^5\text{-}C_5R_4Bz)Fe(CO)Me + CO \quad (3)$$

$$(\eta^5\text{-}C_5R_4Bz)Fe(CO)Me \rightarrow (\eta^5\text{-}C_5R_4CH_2\overline{C_6H_4})Fe(CO)(Me)(H) \quad (4)$$

$$(\eta^5\text{-}C_5R_4CH_2\overline{C_6H_4})Fe(CO)(Me)(H) \rightarrow (\eta^5\text{-}C_5R_4CH_2\overline{C_6H_4})Fe(CO) + CH_4 \quad (5)$$

$$(\eta^5\text{-}C_5R_4CH_2\overline{C_6H_4})Fe(CO) + CO \rightarrow (\eta^5\text{-}C_5R_4CH_2\overline{C_6H_4})Fe(CO)_2 \quad (6)$$

Recent years have seen considerable activity concerning the study of C-H bond activation by transition-metal complexes.[6] This has resulted in the emergence of well-defined stoichiometric reactions which include intramolecular as well as intermolecular oxidative addition of C–H bonds to metal centers, including intermolecular

(1) Blaha, J. P.; Wrighton, M. S. *J. Am. Chem. Soc.* **1985**, *107*, 2694.
(2) Kazlauskas, R. J.; Wrighton, M. S. *Organometallics* **1982**, *1*, 602.
(3) Nelson, G. P.; Wright, M. E. *J. Organomet. Chem.* **1980**, *206*, C21; **1982**, *239*, 353.
(4) Fish, R. W.; Giering, W. P.; Martin, D.; Rosenblum, M. *J. Organomet. Chem.* **1976**, *105*, 111.
(5) Fettes, D. J.; Narayanaswamy, R.; Rest, A. J. *J. Chem. Soc., Dalton Trans.* **1981**, 2311.
(6) (a) Bergman, R. G. *Science (Washington, D.C.)* **1984**, *223*, 901 and references cited therein. (b) Jones, W. D.; Feher, Frank, J. *J. Am. Chem. Soc.* **1985**, *107*, 620 and reference cited therein.

0276-7333/86/2305-0899$01.50/0

Table I. IR and UV-Vis Spectroscopic Data for Relevant Compounds[a]

	temp, K	ν_{CO}, cm^{-1} (ϵ, M^{-1} cm^{-1} or rel abs)	λ_{max}, nm (ϵ, M^{-1} cm^{-1} or rel abs)
$(\eta^5\text{-}C_5H_4Bz)Fe(CO)_2Me$	298	2010 (5500), 1957 (5300)	355 (880), 275 sh
	196	2010 (1.0), 1955 (0.8)	
	77	2009 (1.0), 1952 (0.8)	
$(\eta^5\text{-}C_5Me_4Bz)Fe(CO)_2Me$	298	1995 (9700), 1941 (8800)	355 (1730), 285 sh
	196	1999 (1.0), 1938 (0.9)	
	77	1990 (1.0), 1939 (0.9)	
$(\eta^5\text{-}C_5Me_4Bz)Fe(CO)(^{13}CO)Me$	298	1980 (1.0), 1910 (0.8)	
$(\eta^5\text{-}C_5H_4CH_2\overline{C_6H_4})Fe(CO)_2$	298	2022 (6200), 1973 (7200)	354 (960)
$(\eta^5\text{-}C_5Me_4CH_2\overline{C_6H_4})Fe(CO)_2$	298	2005 (8600), 1955 (10300)	354 (2180)
$(\eta^5\text{-}C_5Me_4Bz)Fe(CO)_2H$	298	2003 (6150), 1945 (6200)	330 (1500)
$(\eta^5\text{-}C_5H_4Bz)Fe(CO)(PPh_3)Me$	298	1917 (3200)	
$(\eta^5\text{-}C_5Me_4Bz)Fe(CO)(PPh_3)Me$	298	1901 (3200)	
$(\eta^5\text{-}C_5H_4CH_2\overline{C_6H_4})Fe(CO)(PPh_3)$	298	1932 (3900)	
$(\eta^5\text{-}C_5Me_4CH_2\overline{C_6H_4})Fe(CO)(PPh_3)$	298	1917 (6500)	
$(\eta^5\text{-}C_5H_4Bz)_2Fe_2(CO)_4$	298	2004 (0.6), 1955 (1.0), 1781 (0.8)	510 (0.2), 400 (0.5), 356 (1.0)
$(\eta^5\text{-}C_5Me_4Bz)_2Fe_2(CO)_4$	298	1931 (1.0), 1762 (0.6)	535 (1500), 420 (3300), 362 (10200)

[a] In deoxygenated methylcyclohexane, Bz = $CH_2C_6H_5$.

Table II. ^1H and ^{13}C NMR Data for Relevant Compounds[a]

	^1H chem shifts, δ vs. $Si(CH_3)_4$	^{13}C chem shifts, δ vs. $Si(CH_3)_4$
$(\eta^5\text{-}C_5H_4Bz)Fe(CO)_2Me$[a]	~7.1 m (5 H), 4.47 t (2 H), 4.44 t (2 H), 3.47 s (2 H), 0.17 s (3 H)	218.8, 218.7 (CO); 140.9, 129.2, 127.1 (phenyl); 106.4, 86.4, 84.8 (Cp); 34.2 (CH_2); -21.2 (Me)
$(\eta^5\text{-}C_5H_4CH_2\overline{C_6H_4})Fe(CO)_2$[b]	6.85 m (1 H), 6.65 m (3 H), 5.02 t (2 H), 4.61 t (2 H), 3.52 s (2 H)	217.5 (CO); 168.2, 155.2, 142.7, 125.7, 125.1, 124.7 (phenyl); 123.2, 84.3, 82.0 (Cp); 34.9 (CH_2)
$(\eta^5\text{-}C_5Me_4Bz)Fe(CO)_2Me$	~7.1 m (5 H), 3.52 s (2 H), 1.72 s (6 H), 1.70 s (6 H), -0.10 s, (3 H)	218.5 (CO); 140.5, 128.9, 128.4, 126.6 (phenyl); 96.6, 95.7, 95.3 (Cp); 31.45 (CH_2); 9.84, 9.50 (CpMe), -13.4 (Me)
$(\eta^5\text{-}Me_4CH_2\overline{C_6H_4})Fe(CO)_2$	6.80 m (1 H), 6.65 m (3 H), 3.45 s (2 H), 1.98 s (6 H), 1.85 s (6 H)	217.7, 216.9 (CO); 164.6, 156.7, 142.9, 125.4, 124.4, 122.9 (phenyl); 119.1, 96.1, 91.0 (Cp); 31.1 (CH_2); 10.1, 9.2 (CpMe)
$(\eta^5\text{-}C_5Me_4Bz)Fe(CO)_2H$	~7.08 m (5 H), 3.70 s (2 H), 1.91 s (6 H), 1.87 s (6 H), -11.8 s (1 H)	
$(\eta^5\text{-}C_5H_4Bz)_2Fe_2(CO)_4$[c]	~7.0 m (5 H), 4.1 s (2 H), 3.64 t (2 H), 3.25 t (2 H)	
$(\eta^5\text{-}C_5Me_4Bz)_2Fe_2(CO)_4$[c]	~7.0 m (5 H), 3.80 s (2 H), 1.72 s (6 H), 1.60 s (6 H)	

[a] In cyclohexane-d_{12}, unless otherwise specified: Bz = $CH_2C_6H_5$; Me = CH_3. [b] ^{13}C NMR was done in acetone-d_6. [c] In benzene-d_6.

C-H addition to soluble complexes of Rh, Ir, and Re.[6-9] A number of reports of intramolecular aromatic C-H additions have been reported.[6b] Perhaps the most relevant result to those detailed here is that near-UV irradiation of $(\eta^5\text{-}C_5H_5)Fe(CO)_2(SiR_3)$ complexes in the presence of PR_3 such as PPh_3 has been noted to yield $(\eta^5\text{-}C_5H_5)\overline{Fe(CO)_2[(C_6H_4)P(C_6H_5)_2]}$ and $HSiR_3$ in unspecified yields.[10]

Experimental Section

Instruments and Equipment. UV-vis spectra were recorded by using a Cary 17 or a Hewlett-Packard 8451A Diode Array spectrophotometer. IR spectra were recorded by using a Nicolet 7199 or a 60SX Fourier transform spectrometer; ^1H and ^{13}C NMR spectra were recorded by using a Bruker 250-MHz (proton) and a Bruker 270-MHz (proton) Fourier transform spectrometer, respectively.

Low-temperature UV-vis and IR spectra were recorded with deoxygenated alkane (methylcyclohexane or 3-methylpentane solution samples held in a Specac Model P/N 21.000 variable-temperature cell with CaF_2 windows, using either liquid N_2 or dry ice/acetone as coolant.

Chemicals. All solvents were reagent grade and freshly distilled before use. Hexane and toluene were distilled from CaH_2 under Ar. Methylcyclohexane (MCH) and tetrahydrofuran (THF) were distilled from Na under Ar. PPh_3 (Aldrich) was recrystallized three times from absolute EtOH. $C_6H_5CH_2Cl$ (Aldrich) and CH_3I (Aldrich) were passed through activated alumina (Woelm Alumina, AKt.I; ICN Nutritional Biochemicals) and deoxygenated before use. Alumina used for chromatography was activated neutral alumina from MCB and used as received. All reactions and manipulations of the organometallic reagents were carried out by using standard Schlenk techniques under an Ar atmosphere or in a Vacuum Atmospheres drybox under Ar. Elemental analyses were done by Schwarzkopf Microanalytical Laboratories, Woodside, NY.

$(\eta^5\text{-}C_5H_4Bz)Fe(CO)_2Me$ was prepared by reaction of $(\eta^5\text{-}C_5H_4Bz)Fe(CO)_2^-$ with CH_3I. A THF solution of 5.4 g (0.01 mol) of $(\eta^5\text{-}C_5H_4Bz)_2Fe_2(CO)_4$ (available from previous synthesis)[1] was reduced by stirring with excess metallic Na (1.0 g, 0.04 mol) to produce $(\eta^5\text{-}C_5H_4Bz)Fe(CO)_2^-$. Upon completion of the reaction

(7) (a) Jones, W. D.; Feher, F. J. *J. Am. Chem. Soc.* **1982**, *104*, 4240-4242. (b) Jones, W. D.; Feher, F. J. *Organometallics* **1983**, *2*, 686-687. (c) Jones, W. D.; Feher, F. J. *J. Am. Chem. Soc.* **1984**, *106*, 1650-1663. (d) Jones, W. D.; Feher, F. J. *Inorg. Chem.* **1984**, *23*, 2376-2388.

(8) (a) Janowicz, A. H.; Bergman, R. G. *J. Am. Chem. Soc.* **1982**, *104*, 352. (b) Jonowicz, A. H.; Bergman, R. G. *J. Am. Chem. Soc.* **1983**, *105*, 3939. (c) Periana, R. A.; Bergman, R. G. *Organometallics* **1984**, *3*, 508. (d) Wax, M. J.; Stryker, J. M.; Buchanan, J. A.; Bergman, R. G. *J. Am. Chem. Soc. 1984, 106*, 7272. (e) Bergman, R. G.; Seidler, P. F.; Wenzel, T. T. *J. Am. Chem. Soc.* **1985**, *107*, 4358. (f) Stoutland, P. O.; Bergman, R. G. *J. Am. Chem. Soc.* **1985**, *107*, 4581.

(9) (a) Hoyano, J. K.; Graham, W. A. G. *J. Am. Chem. Soc.* **1984**, *106*, 1121. (b) Hoyano, J. K.; McMaster, A. D.; Graham, M. A. G. *J. Am. Chem. Soc.* **1984**, *106*, 7190.

(10) Cerveau, G.; Chauviere, G. T.; Colmer, E.; Carriu, R. J. P. *J. Organomet. Chem.* **1981**, *210*, 343.

(as monitored by IR) the excess Na was filtered off and 3.5 g (0.025 mol) of CH_3I was added. After the solution was stirred for 5–10 min, the solvent was stripped off in vacuo and the residue was extracted with hexane. The yellow hexane fraction was concentrated to ~1 mL and chromatographed on an alumina column. Elution with hexane yielded 2.5 g (0.01 mol) of a dark yellow oil. This was further purified by sublimation onto a 196 K probe yielding a bright yellow oil. Spectroscopic data (IR, UV-vis, and NMR) for this and other complexes are found in Tables I and II. Elemental analysis was satisfactory. Anal. Calcd (Found): C, 63.60 (63.45); H, 4.95 (4.65).

(η^5-C_5Me_4Bz)Fe(CO)$_2$Me was prepared in an analogous manner using 6.5 g (0.01 mol) of (η^5-C_5Me_4Bz)$_2$Fe$_2$(CO)$_4$ (prepared by previous synthesis)[1] instead of (η^5-C_5H_4Bz)$_2$Fe$_2$(CO)$_4$. This yielded 3.2 g of (η^5-C_5Me_4Bz)Fe(CO)$_2$)Me as bright yellow crystals. Elemental analysis was satisfactory. Anal. Calcd (Found): C, 67.45 (67.59); H, 6.51 (6.43).

(η^5-C_5Me_4Bz)Fe(CO)$_2$H was prepared by the addition of degassed glacial acetic acid (Aldrich, reagent grade) to a THF solution of (η^5-C_5Me_4Bz)Fe(CO)$_2^-$ (vide supra). The hydride was isolated as a dark yellow oil in a manner analogous to that of (η^5-C_5Me_4Bz)Fe(CO)$_2$Me. Unlike (η^5-C_5H_4Bz)Fe(CO)$_2$H, the (η^5-C_5Me_4Bz)Fe(CO)$_2$H only slowly converts to a Fe–Fe-bonded, (η^5-C_5Me_4Bz)$_2$Fe$_2$(CO)$_4$, species.

Irradiations. A near-UV lamp consisting of two General Electric black light bulbs (355 ± 20 nm, ~2×10^{-6} einstein/min) was used for 298 K irradiations. A 550-W Hanovia medium-pressure Hg lamp was used for preparative photolysis. A Bausch and Lomb SP208 high-pressure Hg lamp (output filtered with Pyrex and ~10 cm of water to remove deep UV and IR light) was used for low-temperature irradiations. Samples of 0.01 M solutions of (η^5-C_5R_4Bz)Fe(CO)$_2$Me in hexanes (with or without 0.05 M PPh_3; 3.0 mL) for quantum yields at 366 nm were freeze–pump–thaw–degassed ($<10^{-5}$ torr, three cycles) in 13 × 100 nm Pyrex test tubes with constrictions and hermetically sealed. Irradiation was carried out in a merry-go-round.[11] The light source for quantum yields was a 550-W medium-pressure Hg lamp (Hanovia) equipped with Corning glass filters to isolate the 366-nm Hg emission. Ferrioxalate actinometry[12] was used to determine excitation rate which was typically ~10^{-7} einstein/min^{-1}. "Flash photolysis" of the hydride (η^5-C_5Me_4Bz)Fe(CO)$_2$H was carried out by using a Xenon Corp. flash photolysis apparatus as a source. A 50-μs flash was used in order to minimize secondary photolysis.

Photoreaction of (η^5-C_5R_4Bz)Fe(CO)$_2$Me. A hexane solution of the complex (R = H) (~0.01 M) was loaded into a Pyrex reaction tube. The photolysis was monitored by removing aliquots for analysis by IR. Upon completion of the reaction, the solvent was stripped off, and the residue was chromatographed on activated alumina. For R = H, the reaction was deemed complete when the oxidative addition product reached a steady-state concentration (about 30% consumption of starting material). The (η^5-$C_5H_4CH_2\overline{C_6H_4}$)Fe(CO)$_2$ undergoes secondary photolysis. Elution with hexane yielded first a yellow band containing the starting material, and then a second yellow band established to be (η^5-$C_5H_4CH_2\overline{C_6H_4}$)Fe(CO)$_2$ by IR and ^{1}H and ^{13}C NMR (Tables I and II). Mass spectrum: M^+ = 267. Anal. Calcd (Found): C, 63.0 (62.86), H, 3.89 (4.10). A red band that remained on the column was eluted with THF and found to be (η^5-C_5H_4Bz)$_2$Fe$_2$(CO)$_4$.

For R = Me, the reaction to form (η^5-$C_5Me_4CH_2\overline{C_6H_4}$)Fe(CO)$_2$ goes to about 95% completion before secondary photolysis becomes important. Chromatography on alumina eluting with hexane yields a yellow band which initially contains traces of starting material. Further elution yields a yellow crystalline material established to be (η^5-$C_5Me_4CH_2\overline{C_6H_4}$)Fe(CO)$_2$ by IR and ^{1}H and ^{13}C NMR (Tables I and II) and X-ray crystallography (vide infra). Mass spectrum M^+ = 322. Anal. Calcd (Found): Fe, 17.35 (17.02); C, 67.11 (66.73); H, 5.59 (5.73). A red band remaining on the column was eluted with THF and found to be (η^5-C_5Me_4Bz)$_2$Fe$_2$(CO)$_4$.

X-ray Crystallography. Crystals of (η^5-$C_5Me_4CH_2\overline{C_6H_4}$)Fe(CO)$_2$ were grown slowly from hexane solutions. X-ray data were collected on an Enraf-Nonious CAD4F-11 diffractometer using MoKα radiation. Data collection, reduction, and refinement procedures have been detailed elsewhere.[13] A total of 3504 reflections ($+h,+k,\pm l$) were collected in the range $3° \le 2\theta \le 55°$ with 2673 having $F_o > 6\sigma(F_o)$ being used in the structure refinement which was by full-matrix least-squares techniques (190 variables) using Shelx-76. Final R_1 = 0.050 and R_2 = 0.073. Hydrogen atoms were ignored and all other atoms were refined anisotropically. An empirical absorption correction was applied. The largest peak in the final-difference Fourier map was 0.68 e Å^{-3}. Table III lists crystal data, Table IV contains selected bond distances and angles, and Table V lists final positional parameters.

Table III. Summary of Crystal Data

(η^5-$C_5Me_5CH_2\overline{C_6H_4}$)Fe(CO)$_2$

a = 9.230 (2) Å	Z = 4
b = 15.321 (4) Å	space group = $P2_1/n$
c = 11.531 (2) Å	mol wt = 332 g
β = 109.76 (1)°	ρ(calcd) = 1.394 g cm^{-3}
V = 1534.6 Å^3	μ = 9.53 cm^{-1}

Table IV. Selected Bond Distances (Å) and Angles (deg)

for (η^5-$C_5Me_4CH_2\overline{C_6H_4}$)Fe(CO)$_2$

Bond Distances

Fe–C1	2.086 (4)	C2–C7	1.520 (5)
Fe–C2	2.118 (3)	C3–C8	1.512 (6)
Fe–C3	2.129 (4)	C4–C9	1.511 (6)
Fe–C4	2.086 (4)	C5–C10	1.512 (6)
Fe–C5	2.073 (4)	C10–C11	1.512 (6)
Fe–C12	1.998 (4)	C11–C12	1.411 (5)
Fe–C17	1.745 (4)	C12–C13	1.388 (5)
Fe–C18	1.752 (4)	C13–C14	1.404 (6)
C1–C2	1.424 (5)	C14–C15	1.388 (7)
C2–C3	1.408 (5)	C15–C16	1.388 (7)
C3–C4	1.451 (6)	C16–C11	1.401 (6)
C4–C5	1.411 (6)	C17–O17	1.154 (5)
C5–C1	1.433 (5)	C18–O18	1.143 (5)
C1–C6	1.503 (5)		

Bond Angles

C1–C2–C3	109.1 (3)	C2–Fe–C12	136.7 (2)
C2–C3–C4	107.3 (4)	C2–Fe–C17	93.3 (2)
C3–C4–C5	107.9 (3)	C2–Fe–C18	131.6 (2)
C4–C5–C1	108.3 (4)	C3–Fe–C4	40.2 (2)
C5–C1–C2	107.4 (3)	C3–Fe–C5	66.8 (2)
C5–C10–C11	107.3 (3)	C3–Fe–C12	145.6 (2)
C10–C11–C12	118.4 (4)	C3–Fe–C17	120.5 (2)
C11–C12–C13	116.4 (3)	C3–Fe–C18	97.8 (2)
C12–C13–C14	121.0 (4)	C4–Fe–C5	39.7 (2)
C13–C14–C15	120.3 (4)	C4–Fe–C12	106.1 (2)
C14–C15–C16	119.7 (4)	C4–Fe–C17	159.3 (2)
C15–C16–C11	119.9 (4)	C4–Fe–C18	94.0 (2)
C16–C11–C12	121.1 (4)	C5–Fe–C12	81.1 (2)
C1–Fe–C2	39.6 (1)	C5–Fe–C17	137.1 (2)
C1–Fe–C3	66.4 (2)	C5–Fe–C18	124.9 (2)
C1–Fe–C4	67.1 (2)	C12–Fe–C17	91.3 (2)
C1–Fe–C5	40.3 (2)	C12–Fe–C18	90.2 (2)
C1–Fe–C12	97.3 (2)	C17–Fe–C18	97.1 (2)
C1–Fe–C17	100.2 (2)	Fe–C5–C10	116.1 (3)
C1–Fe–C18	160.9 (2)	Fe–C12–C11	116.4 (3)
C2–Fe–C3	38.7 (1)	Fe–C12–C13	125.6 (3)
C2–Fe–C4	66.4 (2)	Fe–C17–O17	177.7 (4)
C2–Fe–C5	66.7 (2)	Fe–C18–O18	177.4 (4)

Results

a. Room-Temperature Irradiation of (η^5-C_5R_4Bz)-Fe(CO)$_2$Me. Near-UV irradiation of a 0.01 M alkane solution of (η^5-C_5R_4Bz)Fe(CO)$_2$Me (R = H, Me) at 298 K

(11) Moses, F. G.; Lui, R. S. H.; Monroe, B. M. *Mol. Photochem.* **1969**, *1*, 245.

(12) Hatchard, C. G.; Parker, C. A. *Proc. R. Soc. London, Ser. A* **1956**, *234*, 518.

(13) Silverman, L. D.; Dewan, J. C.; Giandomenico, C. M.; Lippard, S. J. *Inorg. Chem.* **1980**, *19*, 3379.

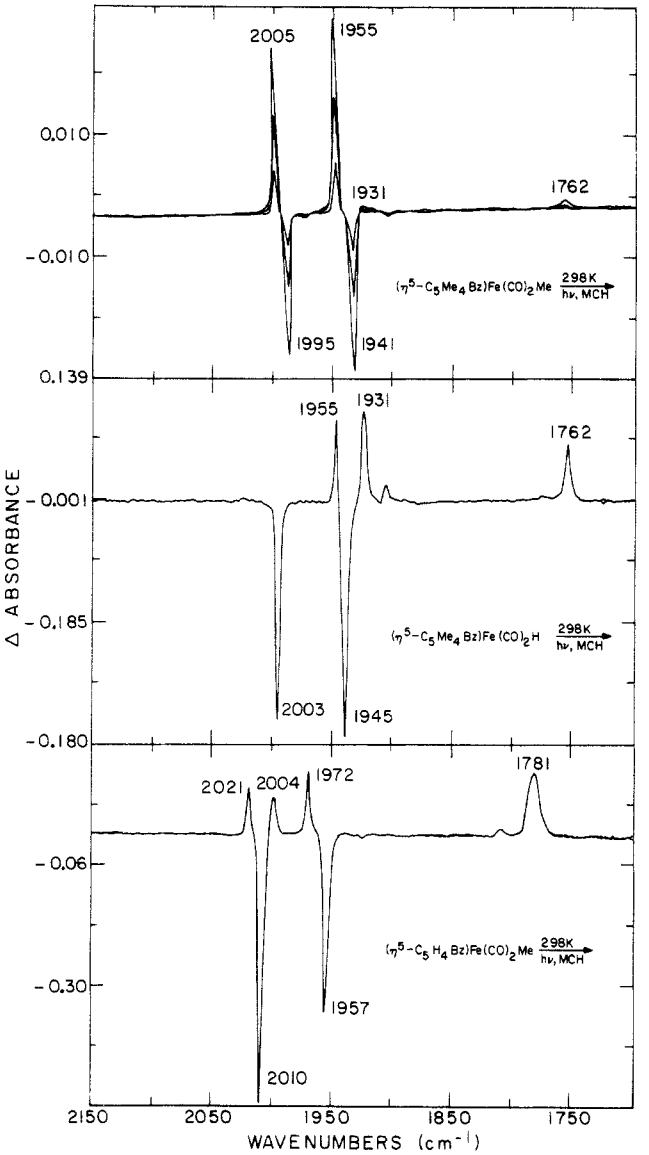

Figure 1. IR spectral changes (difference spectra) accompanying near-UV irradiation of ~0.01 M metal complex in deoxygenated solution. Negative peaks correspond to consumed starting materials and positive peaks correspond to products. Top: 2005 and 1955 cm^{-1} correspond to $(\eta^5\text{-}C_5Me_4CH_2\overline{C_6H_4})Fe(CO)_2$ and 1931 and 1762 cm^{-1} correspond to $(\eta^5\text{-}C_5Me_4Bz)_2Fe_2(CO)_4$. Middle: 1955 cm^{-1} is due to $(\eta^5\text{-}C_5Me_4CH_2\overline{C_6H_4})Fe(CO)_2$ (the 2005 cm^{-1} peak is obscured by the 2003 cm^{-1} peak of starting material) and 1931 and 1762 cm^{-1} correspond to $(\eta^5\text{-}C_5Me_4Bz)_2Fe_2(CO)_2$. Bottom: 2021 and 1972 cm^{-1} are due to $(\eta^5\text{-}C_5H_4CH_2\overline{C_6H_4})Fe(CO)_2$ and 2004 and 1781 cm^{-1} are due to $(\eta^5\text{-}C_5H_4Bz)_2Fe_2(CO)_4$.

results in IR changes shown in Figure 1. In all cases, the decline of the starting material bands and the growth of IR bands attributable to the expected[1] $(\eta^5\text{-}C_5R_4Bz)_2Fe_2(CO)_4$ are observed with increasing irradiation time. The interesting new photoreaction is represented by eq 7.

$$(\eta^5\text{-}C_5R_4Bz)Fe(CO)_2Me \xrightarrow[h\nu,\ MCH]{298\ K} (\eta^5\text{-}C_5R_4CH_2\overline{C_6H_4})Fe(CO)_2 + CH_4 \quad (7)$$

R = H, Me

Figure 1 (top) shows the decline of the starting material bands for R = Me with concomitant growth of $(\eta^5\text{-}C_5Me_4CH_2\overline{C_6H_4})Fe(CO)_2$ absorption at 2005 and 1955 cm^{-1} and of $(\eta^5\text{-}C_5Me_4Bz)_2Fe_2(CO)_4$ absorption at 1931 and 1762 cm^{-1}. For R = H, Figure 1 (bottom), the oxidative addition

Table V. Final Positional Parameters for the Atoms of $(\eta^5\text{-}C_5Me_4CH_2\overline{C_6H_4})Fe(CO)_2$[a]

atom	x	y	z
Fe	0.22573 (6)	−0.06222 (3)	0.33270 (4)
C1	0.1227 (5)	−0.0613 (3)	0.1414 (3)
C2	0.2539 (5)	−0.0057 (3)	0.1741 (3)
C3	0.2348 (5)	0.0614 (3)	0.2511 (4)
C4	0.0877 (5)	0.0472 (3)	0.2678 (4)
C5	0.0195 (5)	−0.0273 (3)	0.1993 (3)
C6	0.0904 (6)	−0.1391 (3)	0.0572 (4)
C7	0.3883 (6)	−0.0147 (3)	0.1269 (4)
C8	0.3412 (6)	0.1372 (3)	0.3048 (4)
C9	0.0148 (6)	0.1065 (3)	0.3374 (5)
C10	−0.1221 (5)	−0.0753 (3)	0.2030 (5)
C11	−0.0679 (5)	−0.1486 (3)	0.2954 (4)
C12	0.0894 (4)	−0.1521 (2)	0.3681 (3)
C13	0.1371 (5)	−0.2182 (3)	0.4550 (4)
C14	0.0330 (6)	−0.2812 (3)	0.4677 (4)
C15	−0.1209 (6)	−0.2778 (3)	0.3940 (4)
C16	−0.1720 (5)	−0.2113 (3)	0.3079 (4)
C17	0.3704 (5)	−0.1393 (3)	0.3491 (4)
C18	0.2858 (5)	−0.0281 (3)	0.4868 (4)
O17	0.4639 (4)	−0.1909 (2)	0.3559 (3)
O18	0.3197 (4)	−0.0044 (3)	0.5864 (3)

[a] Numbers in parentheses are errors in the last significant digit(s).

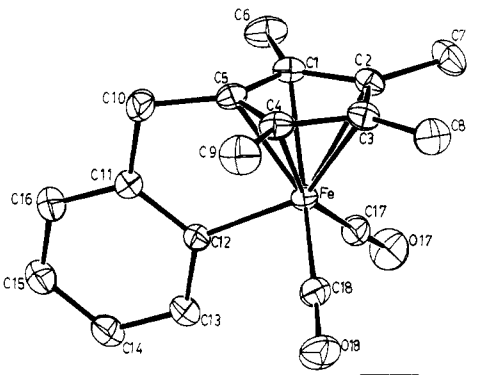

Figure 2. Ortep diagram of $(\eta^5\text{-}C_5Me_4CH_2\overline{C_6H_4})Fe(CO)_2$. The ellipsoids correspond to 30% probability.

product $(\eta^5\text{-}C_5H_4CH_2\overline{C_6H_4})Fe(CO)_2$ absorbs at 2021 and 1972 cm^{-1} and the dimeric product $(\eta^5\text{-}C_5H_4Bz)_2Fe_2(CO)_4$ absorbs at 2004 and 1955 cm^{-1} (obscured by starting material absorption) and 1781 cm^{-1}. Interestingly, the hydride $(\eta^5\text{-}C_5Me_4Bz)Fe(CO)_2H$ also gives the oxidative addition compound $(\eta^5\text{-}C_5Me_4CH_2\overline{C_6H_4})Fe(CO)_2$ on photolysis (Figure 1 (middle)), albeit in smaller yield, along with the $(\eta^5\text{-}C_5Me_4Bz)_2Fe_2(CO)_4$ dimer.

When the photoreaction of $(\eta^5\text{-}C_5R_4Bz)Fe(CO)_2Me$ is monitored by ^1H NMR, quantitative evolution of CH_4 is observed along with the growth of the oxidative addition product. The CH_4 resonance is a sharp singlet at 0.18 ppm in cyclohexane-d_{12}. The fact that this resonance is a sharp singlet rules out the role of the deuterated solvent as a hydrogen source and is consistent with an intramolecular pathway for hydrogen abstraction by the Me group. Interestingly, near-UV photolysis of 0.01 M $(\eta^5\text{-}C_5Me_5)Fe(CO)_2Me$ in benzene yields no CH_4 and no oxidative addition product analogous to that obtained from the $(\eta^5\text{-}C_5R_4Bz)Fe(CO)_2Me$ under the same conditions.

Characterization and Structure of $(\eta^5\text{-}C_5R_4CH_2\overline{C_6H_4})Fe(CO)_2$. The interesting new photoproducts $(\eta^5\text{-}C_5R_4CH_2\overline{C_6H_4})Fe(CO)_2$ from the $(\eta^5\text{-}C_5R_4Bz)Fe(CO)_2R'$ precursors have been fully characterized, and for R = Me an X-ray structure provides unequivocal proof of structure (Figure 2). The elemental analyses and mass spectrometry results (cf. Experimental Section) are in accord with the

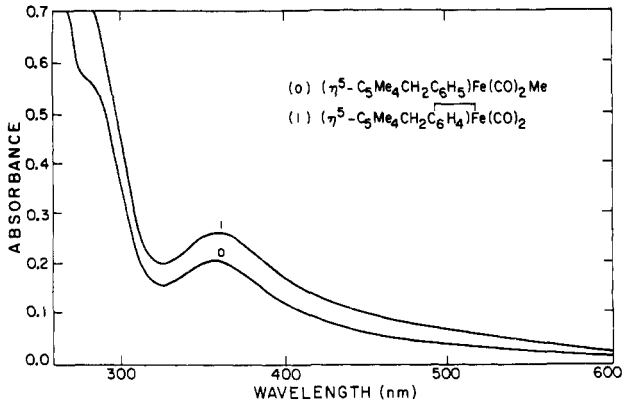

Figure 3. UV–vis spectra of $\sim 10^{-3}$ M alkane solutions of (η^5-C_5Me_4Bz)$Fe(CO)_2Me$ and of (η^5-$C_5Me_4CH_2\overline{C_6H_4}$)$Fe(CO)_2$ in 1.0-mm path length quartz cells.

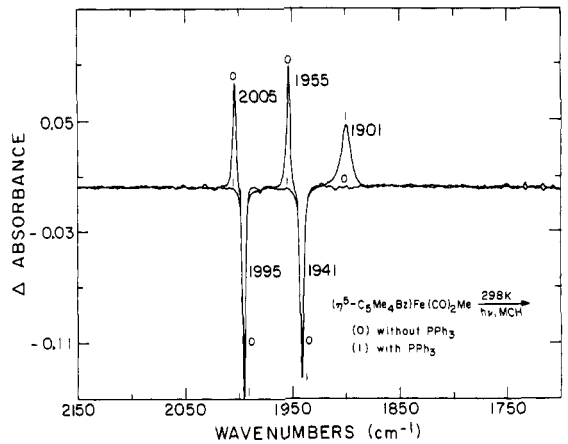

Figure 4. Comparison of the IR difference spectra upon near-UV irradiation of 0.01 M alkane solution of (η^5-C_5Me_4Bz)$Fe(CO)_2Me$ at 298 K with (trace 1) and without (trace 0) 0.05 M PPh_3 after 45 s of irradiation. The peak at 1901 cm^{-1} corresponds to (η^5-C_5Me_4Bz)$Fe(CO)(PPh_3)Me$ while those at 2005 and 1955 cm^{-1} correspond to (η^5-$C_5Me_4CH_2\overline{C_6H_4}$)$Fe(CO)_2$.

composition given in eq 7, and IR and UV–vis spectral data (Table I) and ^1H and ^{13}C NMR (Table II) are consistent with the molecular structure shown in Figure 2. Tables III–V give data relevant to the X-ray crystallography.

The two CO stretching absorptions in the IR for the dicarbonyl product are at higher frequency than in the starting Me complexes, presumably due to the π-back-bonding capability in the σ-phenyl system which is not present for the Me species. The relative intensity of the two CO bands is roughly that expected on the basis of the OC–Fe–CO angle. The geometrical arrangement of the (η^5-$C_5Me_4CH_2\overline{C_6H_4}$)$Fe(CO)_2$ is similar to that for other such complexes,[14] but the C_5 ring carbons are not equidistant from the Fe. However, the C_5 ring is planar with deviations from the least-squares plane through atoms C1–C5 ranging from 0.000 to 0.0006Å. Atoms C6–C9 lie between 0.04 and 0.08 Å above this plane while atom C10 lies 0.20 Å below the plane. Interestingly, the (η^5-$C_5R_4CH_2\overline{C_6H_4}$)$Fe(CO)_2$ species have UV–vis spectra that are not very different from those for the starting Me complexes (Figure 3). The tilt of the C_5 ring might be expected to give a red shift of the first ligand field absorption, as has been observed in certain ferrocenophanes.[15] Apparently, offsetting factors keep the first absorption at about the same energy as in the starting Me species.

The ^1H and ^{13}C NMR data (Table II) also accord well with the X-ray structure. The ^1H NMR is consistent with the geometrical formulation. Notably, the phenyl region shows two multiplets in a 1:3 ratio. In analogy to related systems[16] and from the integration, the lower field multiplet at 6.80 ppm for R = H and 6.85 ppm for R = Me is assigned to the ortho H. The ^1H-decoupled ^{13}C NMR shows six carbon resonances in the phenyl region, as expected. An unambiguous assignment of the phenyl resonances is not possible from these data, but the ^1H coupled spectrum shows that two of the resonances, 168.2 and 155.2 ppm for R = H and 164.6 and 156.7 ppm for R = Me, remain as singlets. These singlets are assigned to the phenyl C bonded to the Fe and to the phenyl C bonded to the CH_2. Tentatively, by comparison with other systems[16,17] we assign the lower field of the two singlets to the phenyl C directly bonded to Fe.

Quantum Yields for Photoreaction of (η^5-C_5R_4Bz)$Fe(CO)_2Me$ with and without PPh_3 or CO. In the presence of 0.05 M PPh_3, irradiation of 0.01 M alkane solution of (η^5-C_5R_4Bz)$Fe(CO)_2Me$ yields no oxidative addition products. Instead, a nearly quantitative conversion to (η^5-C_5R_4Bz)$Fe(CO)(PPh_3)Me$ and a small (<5%) amount of (η^5-C_5R_4Bz)$_2Fe_2(CO)_2$ is observed. The (η^5-$C_5R_4CH_2\overline{C_6H_4}$)$Fe(CO)_2$ complexes are, not surprisingly,[1] photosensitive with respect to CO loss. This fact has been exploited to prepare (η^5-$C_5R_4CH_2\overline{C_6H_4}$)$Fe(CO)PPh_3$ by irradiation of (η^5-$C_5R_4CH_2\overline{C_6H_4}$)$Fe(CO)_2$ in the presence of PPh_3. The (η^5-$C_5R_4CH_2\overline{C_6H_4}$)$Fe(CO)PPh_3$ has a single CO absorption in the IR at higher energy than for (η^5-C_5R_4Bz)$Fe(CO)(PPh_3)Me$. The spectral differences allow the conclusion that (η^5-C_5R_4Bz)$Fe(CO)(PPh_3)Me$, not (η^5-$C_5R_4CH_2\overline{C_6H_4}$)$Fe(CO)PPh_3$, is the photoproduct from irradiation of (η^5-C_5R_4Bz)$Fe(CO)_2Me$ in the presence of 0.05 M PPh_3. By ^1H NMR, there is no CH_4 evolved, consistent with suppressing the oxidative addition/reductive elimination process giving CH_4 in the absence of PPh_3. Figure 4 shows the IR spectral changes associated with the near-UV irradiation of a 0.01 M alkane solution (η^5-C_5Me_4Bz)$Fe(CO)_2Me$ with (trace 0) and without (trace 1) 0.05 M PPh_3. We obtain very similar values for the disappearance quantum yields ϕ_{366nm} for (η^5-C_5Me_4Bz)$Fe(CO)_2Me$ with 0.05 M PPh_3 ($\phi_{366nm} = 0.46$) and without PPh_3 ($\phi_{366nm} = 0.40$) at the same excitation rate, $\sim 3 \times 10^{-5}$ M/min. We have avoided potential problems from secondary photolysis by making quantum yield determinations at very low (≤10%) extent conversion. These results indicate that dissociative loss of CO is the principal result of photoexcitation and that the oxidative addition of the ortho C–H bond follows this reaction. PPh_3, however, is an extremely efficient 2e trap for the CO loss product and even at relatively low concentrations ($\sim 2 \times 10^{-3}$) is able to suppress the oxidative addition. Apparently the rate for the two-step process (eq 4 and 5) of oxidative addition and reductive elimination of CH_4 is so small that formation of an oxidative addition product is suppressed at relatively low PPh_3 concentration. However, reaction of (η^5-C_5Me_4Bz)$Fe(CO)Me$ with the photoejected CO is not

(14) Bennett, M. J.; Cotton, F. A.; Davison, A.; Faller, J. W.; Lippard, S. J.; Morehouse, S. M. *J. Am. Chem. Soc.* **1966**, *88*, 4371 and references therein.

(15) Fischer, A. B.; Kinney, J. B.; Staley, R. H.; Wrighton, M. S. *J. Am. Chem. Soc.* **1979**, *101*, 6501.

(16) (a) Stewart, R. P., Jr.; Isbrandt, L. R.; Benedict, J. J.; Palmer, J. G. *J. Am. Chem. Soc.* **1976**, *98*, 3215. (b) McKinney, R. J.; Haxmeier, R.; Kaesz, H. D. *J. Am. Chem. Soc.* **1975**, *97*, 3059. (c) Ahmad, N.; Ainscough, E. W.; James, T. A.; Robinson, S. O. *J. Chem. Soc., Dalton Trans.* **1973**, 1151.

(17) Kohler, F. H.; Matsubayashi, G. E. *J. Organomet. Chem.* **1975**, *96*, 391.

competitive with oxidative addition of the ortho C–H bond at an excitation rate of $\sim 3 \times 10^{-5}$ M/min.

The results on photosubstitution are consistent with previous findings concerning the photochemistry of (η^5-C_5R_5)Fe(CO)$_2$R′ (R = H, CH$_3$; R′ = CH$_3$, Bz).[1,2] In the presence of PPh$_3$ the 366-nm disappearance quantum yield for R = CH$_3$ and R′ = Bz is 0.35 which contrasts with a smaller 366-nm disappearance quantum yield of ~0.10 in the absence of PPh$_3$ but under otherwise identical conditions.[1,2] In the presence of PPh$_3$ the simple substitution product (η^5-C_5R_5)Fe(CO)(PPh$_3$)R is formed with high quantum efficiency; in the absence of PPh$_3$, back reaction with CO occurs to give less net chemical reaction, except (η^5-C_5R_5)$_2$Fe$_2$(CO)$_4$ formation via a less efficient path stemming from photochemical formation of benzyl radicals. For (η^5-C_5Me_4Bz)Fe(CO)$_2$Me, however, the 366-nm disappearance quantum yield in the absence of PPh$_3$ is in close agreement with the disappearance in the presence of PPh$_3$. Apparently, in the absence of PPh$_3$ as a trap, the ortho C–H bond of the phenyl ring of (η^5-C_5Me_4Bz)Fe(CO)$_2$Me serves as a trap and precludes efficient back reaction with CO to regenerate starting material at low excitation rate where the steady-state concentration of CO is low.

For (η^5-C_5H_4Bz)Fe(CO)$_2$Me the disappearance quantum yield without PPh$_3$ is 0.08, much lower than the disappearance quantum yield of 0.65 with 0.05 M PPh$_3$. The yield for the oxidative addition reaction is much lower than for photosubstitution. Evidently, back reaction of (η^5-C_5H_4Bz)Fe(CO)Me with the photoejected CO is very competitive with the two-step process of oxidative addition of the ortho C–H bond followed by elimination of CH$_4$.

The difference in quantum yield between the (η^5-C_5Me_4Bz)Fe(CO)$_2$Me and (η^5-C_5H_4Bz)Fe(CO)$_2$Me for formation of (η^5-$C_5R_4CH_2\overline{C_6H_4}$)Fe(CO)$_2$ could be due to the better electron-releasing properties of the C_5Me_4Bz ligand. Electron-releasing ligands are known to favor oxidative addition reaction.[18] However, other equally important factors cannot be ruled out. The rate of CO back reaction (or, reaction with a 2e ligand such as PPh$_3$) may be much higher for (η^5-C_5H_4Bz)Fe(CO)Me than for (η^5-C_5Me_4Bz)Fe(CO)Me, such that CO back reaction competes seriously with the oxidative addition reaction in one case and not the other. Indeed, the more hindered (η^5-C_5Me_4Bz)Fe(CO)Me would be expected to react more slowly with incoming ligands than the R = H analogue. In any event, the net difference in photoreactivity is fairly modest, since the quantum yields in the absence of added ligands differ by a factor of less than 10.

Like added PPh$_3$, added CO suppresses the oxidative addition reaction of (η^5-C_5R_4Bz)Fe(CO)$_2$Me. For example, when (η^5-C_5Me_4Bz)Fe(CO)$_2$Me is irradiated in the presence of 4×10^{-3} M ^{13}CO no oxidative addition product is observed. Rather, the ^{13}CO-monosubstituted complex (η^5-C_5Me_4Bz)Fe(CO)(^{13}CO)Me is formed (Figure 5). When natural abundance CO is used, the 4×10^{-3} M CO efficiently suppresses formation of (η^5-$C_5Me_4CH_2\overline{C_6H_4}$)Fe(CO)$_2$. In the ^{13}CO experiments it is noteworthy that (η^5-$C_5Me_4CH_2\overline{C_6H_4}$)Fe(CO)(^{13}CO) is not observed as a primary product at a ^{13}CO concentration as low as 1×10^{-3} M. Comparisons of the trapping efficiency by CO and PPh$_3$ are difficult to interpret, owing to differences in their steric demands, and quantitative results must await direct measurement of rate constants.

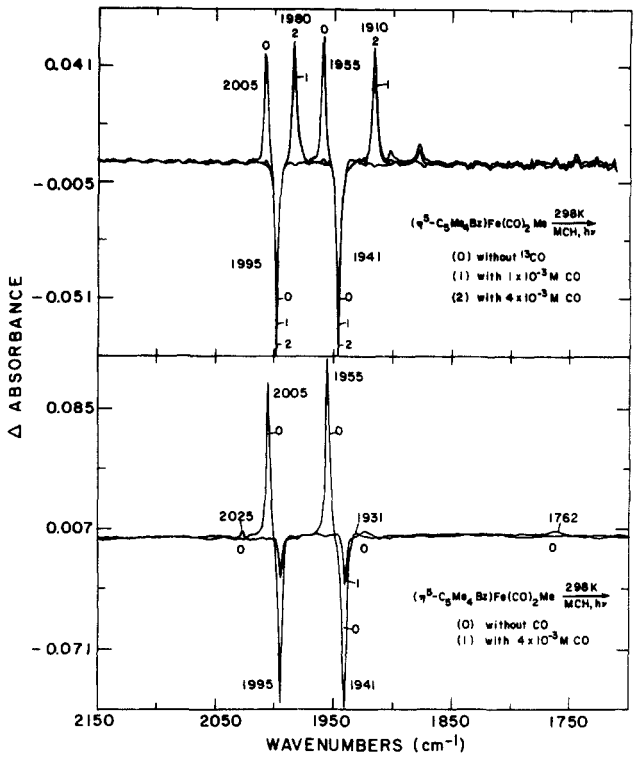

Figure 5. Top: Difference IR spectra obtained upon near-UV irradiation of (η^5-C_5Me_4Bz)Fe(CO)$_2$Me without (trace 0) and with (traces 1 and 2) ^{13}CO after 15 s of irradiation. The negative peaks correspond to bands due to the disappearance of (η^5-C_5Me_4Bz)Fe(CO)$_2$Me. For trace 0, the peaks at 2005 and 1955 cm^{-1} are due to the oxidative addition product (η^5-$C_5Me_4CH_2\overline{C_6H_4}$)Fe(CO)$_2$. For traces 1 and 2, the peaks at 1980 and 1910 cm^{-1} are due to (η^5-C_5Me_4Bz)Fe(CO)(^{13}CO)Me. Bottom: difference IR spectra of (η^5-C_5Me_4Bz)Fe(CO)$_2$Me without (trace 0) and with (trace 1) 4×10^{-3} M CO after 15 s of irradiation. For trace 0, the product peaks at 2005 and 1955 cm^{-1} are due to (η^5-$C_5Me_4CH_2\overline{C_6H_4}$)Fe(CO)$_2$ while for trace 1, the small product peak at 2025 cm^{-1} corresponds to (η^4-C_5Me_5Bz)Fe(CO)$_3$ and those at 1931 and 1762 cm^{-1} correspond to (η^5-C_5Me_4Bz)$_2$Fe$_2$(CO)$_4$.

The photochemistry of (η^5-C_5R_4Bz)Fe(CO)$_2$Me under 30 psi of CO parallels that observed for (η^5-C_5R_5)Fe(CO)$_2$R′ (R = H, Me; R′ = Bz, Me). For R = H, the CO insertion product (η^5-C_5H_4Bz)Fe(CO)(COMe) forms thermally at 298 K as is the case for (η^5-C_5H_5)Fe(CO)$_2$Me.[1] IR bands consistent with the formation of a diene iron tricarbonyl, (η^4-C_5Me_5Bz)Fe(CO)$_3$, are observed, along with bands characteristic of (η^5-C_5Me_5Bz)$_2$Fe$_2$(CO)$_4$ upon irradiation of (η^5-C_5Me_4Bz)Fe(CO)$_2$Me in alkane solution under 30 psi of CO. These results are in agreement with previous findings in this laboratory which show that cyclopentadiene iron tricarbonyls (η^4-C_5Me_5R')Fe(CO)$_3$ (R′ = Me, Bz) are formed from the reaction of photogenerated (η^5-C_5Me_5)Fe(CO)$_2$ and R′ radicals under CO.[1]

b. Low-Temperature Photochemistry of (η^5-C_5R_4Bz)Fe(CO)$_2$Me. Low-temperature photolysis of (η^5-C_5R_4Bz)Fe(CO)$_2$Me was carried out with the aim of detecting any of the possible monocarbonyl intermediates, (η^5-C_5R_4Bz)Fe(CO)Me, (η^5-$C_5R_4CH_2\overline{C_6H_4}$)Fe(CO)(H)(Me), or ($\eta^5$-$C_5R_4CH_2\overline{C_6H_4}$)Fe(CO) along the path to (η^5-$C_5R_4CH_2\overline{C_6H_4}$)Fe(CO)$_2$. Near-UV irradiation of 0.01 M (η^5-C_5R_4Bz)Fe(CO)$_2$Me in a methylcyclohexane matrix at 77 K yields no photoreaction. In a 1-pentene matrix at 77 K for R = H, however, spectral changes associated with the formation of a 1-pentene substitution complex, (η^5-

(18) Collman, J. P.; Hegedus, L. S. "Principles and Applications of Organotransition Metal Chemistry"; University Science Books: Mill Valley CA, 1980.
(19) (a) Randolph, C. L.; Wrighton, M. S. *J. Am. Chem. Soc.*, in press. (b) Randolph, C. L. Ph.D. Thesis, M.I.T., 1985.

Scheme I

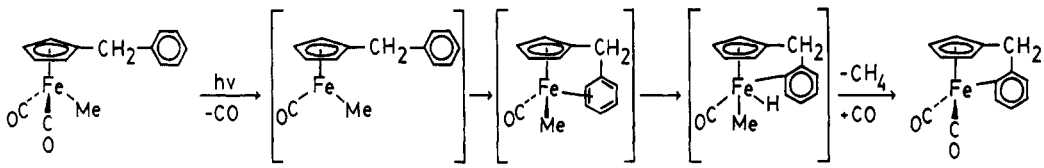

$C_5H_4Bz)Fe(CO)(Me)$(1-pentene), along with the growth of free CO at 2132 cm^{-1} are observed. Photoreaction in 1-pentene but not in methycyclohexane is consistent with findings concerning the 77 K photochemistry of $(\eta^5$-$C_5H_5)Fe(CO)_2Me$.[2] Apparently, reversibility of CO loss in the absence of a trap precludes detection of a monocarbonyl, $(\eta^5$-$C_5H_4Bz)Fe(CO)Me$, species. For $(\eta^5$-$C_5Me_4Bz)Fe(CO)_2Me$ a 1-pentene-substituted complex was obtained only after prolonged photolysis (~2 h), at an extremely low extent conversion (<0.1%). The corresponding $(\eta^5$-$C_5Me_5)Fe(CO)_2Me$ behaves similarly under these conditions. At 196 K, however, photolysis of $(\eta^5$-$C_5R_4Bz)Fe(CO)_2Me$ (R = H, Me) in 1-pentene leads to rapid conversion to $(\eta^5$-$C_5R_4Bz)Fe(CO)$(1-pentene)Me. Photolysis of $(\eta^5$-$C_5R_4Bz)Fe(CO)_2Me$ in alkane solutions at 196 K leads to complete conversion to $(\eta^5$-$C_5R_4CH_2\overline{C_6H_4})Fe(CO)_2$, and no intermediates can be detected. Thus, low-temperature studies (down to ~77 K) fail to allow detection and characterization of the intermediates involved in photochemistry according to eq 7.

c. Photoreaction of $(\eta^5$-$C_5Me_4CH_2\overline{C_6H_4})Fe(CO)_2$ under H_2 or D_2. A $(\eta^5$-$C_5Me_4Bz)$ complex can be regenerated by photoreaction of $(\eta^5$-$C_5Me_4CH_2\overline{C_6H_4})Fe(CO)_2$ under H_2 or D_2. Figure 6 shows IR spectral changes observed upon flash photolysis of a 0.01 M alkane solution of $(\eta^5$-$C_5Me_4CH_2\overline{C_6H_4})Fe(CO)_2$ saturated with H_2. There is a decline of the two bands due to the starting material and a growth of bands attributed to $(\eta^5$-$C_5Me_4Bz)Fe(CO)_2H$ (2005, 1940 cm^{-1}) and to the dimer $(\eta^5$-$C_5Me_4Bz)_2Fe_2(CO)_4$ (1932, 1762 cm^{-1}). A distinct Fe–H peak is observed at −11.8 ppm when the reaction is monitored by ^1H NMR in cyclohexane-d_{12}. Flash photolysis of a cyclohexane solution of $(\eta^5$-$C_5Me_4CH_2\overline{C_6H_4})Fe(CO)_2$ saturated with D_2 yields $(\eta^5$-$C_5Me_4CH_2C_6H_4D)Fe(CO)_2D$ as evidenced by ^2H NMR: a peak at −11.8 ppm is attributed to the deuteride and a peak at 7.02 ppm, an aromatic resonance, is attributed to the ortho deuterium of the benzyl group. The inability to integrate the ^2H NMR (low signal to noise) does not unambiguously allow us to conclude that both ortho positions of the benzyl group are deuterated. However, since irradiation of $(\eta^5$-$C_5Me_4Bz)Fe(CO)_2H$ yields some $(\eta^5$-$C_5Me_4CH_2\overline{C_6H_4})Fe(CO)_2$ (vide supra, Figure 1 (middle)), it is likely that both ortho positions can be deuterated. The results at least show that the cyclometallation can be reversed. The photochemical formation of $(\eta^5$-$C_5Me_4Bz)Fe(CO)_2H$ from $(\eta^5$-$C_5Me_4CH_2\overline{C_6H_4})Fe(CO)_2$ under H_2 presumably begins with the loss of CO followed by addition of H_2 to form $(\eta^5$-$C_5Me_4CH_2\overline{C_6H_4})Fe(CO)(H)(H)$. Formation of $(\eta^5$-$C_5Me_4Bz)Fe(CO)_2H$ can then occur by reductive elimination of the ortho C–H bond followed by uptake of CO.

Discussion

Our work on the $(\eta^5$-$C_5R_4Bz)Fe(CO)_2Me$ systems is consistent with the results that we have gathered from previous work on the photochemistry of $(\eta^5$-$C_5R_5)Fe(CO)_2R'$.[1,2] The primary results of the excited-state decay

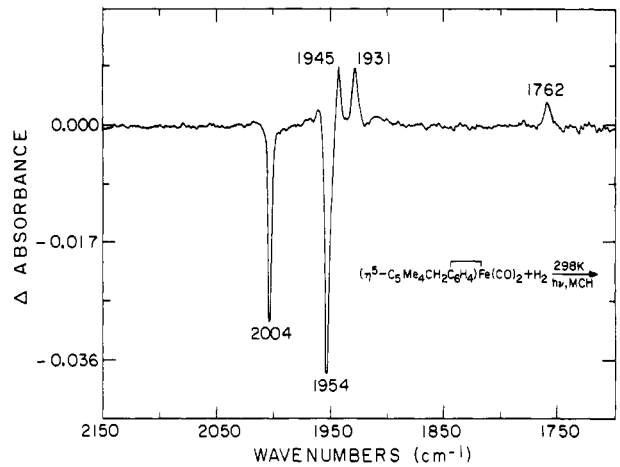

Figure 6. Difference IR spectrum upon flash photolysis of a H_2-saturated alkane solution of $(\eta^5$-$C_5Me_4CH_2\overline{C_6H_4})Fe(CO)_2$. The bands at 2003 (obscured by starting material) and 1945 cm^{-1} are due to $(\eta^5$-$C_5Me_4Bz)Fe(CO)_2H$ while those at 1931 and 1762 cm^{-1} are due to $(\eta^5$-$C_5Me_4Bz)_2Fe_2(CO)_4$.

from the near-UV photolysis of $(\eta^5$-$C_5R_5)Fe(CO)_2R'$ are dissociative loss of CO which occurs with high quantum yield and Fe–R′ homolysis to yield radical products which occurs with low quantum yield. For $(\eta^5$-$C_5R_5)Fe(CO)_2R'$ we did not observe any net chemical yield for the CO loss pathway in alkanes due to back reaction of the 16e $(\eta^5$-$C_5R_5)Fe(CO)R'$ with CO; for $(\eta^5$-$C_5R_4Bz)Fe(CO)_2Me$, however, we are able to obtain cyclometalated products resulting from the oxidative addition of the benzyl ortho C–H bond to the metal center of the CO loss product. Apparently, the two-step process of oxidative addition of the ortho C–H bond and elimination of CH_4 occurs faster than back reaction with CO. However, PPh_3 or added CO at low concentration can efficiently capture the CO loss product and suppress the oxidative addition process completely. The mechanism for the chemistry according to eq 7 is likely the sequence given by eq 3–6. Unfortunately, none of the intermediates in the photoreaction can be detected, even at low temperature. The CO loss product, though, $(\eta^5$-$C_5R_4Bz)Fe(CO)Me$ is efficiently scavenged by added 2e donor ligands. The voracity of the 16e species with respect to ligand uptake suggests that an η^2-phenyl species may precede oxidative addition of the ortho C–H as illustrated in Scheme I. However, such an interaction apparently is not effective in "trapping" the CO loss product from $(\eta^5$-$C_5H_4Bz)Fe(CO)_2Me$, because there is no reaction in an alkane matrix at 77 K. The formation of an η^2-phenyl species apparently precedes oxidative addition of arenes to Rh,[6b] but oxidative addition of C_2H_4 to Ir does not involve a prior η^2-C_2H_4 complex.[8f] In the case at hand the η^2-phenyl species, if important, is labile.

The reversion of the proposed intermediate $(\eta^5$-$C_5R_4CH_2\overline{C_6H_4})Fe(CO)(Me)(H)$ to $(\eta^5$-$C_5R_4Bz)Fe(CO)Me$, the reverse of eq 4, is possible considering the results from irradiation of $(\eta^5$-$C_5Me_4CH_2\overline{C_6H_4})Fe(CO)_2$ under H_2 or D_2. However, elimination of CH_4 from $(\eta^5$-$C_5R_4CH_2\overline{C_6H_4})Fe(CO)(Me)(H)$, eq 5, is likely irreversible: we have obtained

no evidence for intermolecular oxidative addition of C–H bonds to (η^5-C_5R_5)Fe(CO)R′ species. The oxidative addition of any C–H bond to the photogenerated 16e (η^5-C_5R_5)Fe(CO)R′ species actually has little precedent,[10] but there is much literature showing that intramolecular C–H addition processes can be more facile than intermolecular processes.[6b] The photoreaction of (η^5-$C_5Me_4CH_2\overline{C_6H_4}$)-$\overline{Fe(CO)_2}$ under H_2 shows that oxidative addition/reductive elimination processes are viable, and recent work[19] shows that (η^5-C_5Me_5)Fe(CO)$_2$Me yields (η^5-C_5Me_5)Fe(CO)$_2$SiMe$_3$ when irradiated in the presence of Me_3SiH. Elaboration of the scope of photoinduced C–H addition processes in the (η^5-C_5R_5)Fe(CO)$_2$R′ system will be attempted in this laboratory.

Acknowledgment. We thank the National Science Foundation for support of this research. We also thank the Biomedical Research Support Shared Instrumentation Grant Program, Division of Research Resources, for funds to purchase the X-ray diffraction equipment (NIH Grant S10RR02243-01). We thank the M.I.T. Mass Spectrometry Facility and the M.I.T. Spectrometry Laboratory for mass spectrometry. The M.I.T. Mass Spectrometry Facility is supported by the National Institutes of Health Research Grant No. RR0317 from the Biotechnology Resources Branch, Division of Research Resources.

Registry No. (η^5-C_5H_4Bz)Fe(CO)$_2$Me, 100909-58-8; (η^5-C_5Me_4Bz)Fe(CO)$_2$Me, 100909-59-9; (η^5-C_5H_4Bz)$_2$Fe$_2$(CO)$_4$, 95585-27-6; (η^5-C_5Me_4Bz)$_2$Fe$_2$(CO)$_4$, 95420-99-8; (η^5-C_5Me_4Bz)-Fe(CO)$_2$H, 100909-60-2; (η^5-$C_5H_4CH_2\overline{C_6H_4}$)Fe(CO)$_2$, 100909-61-3; ($\eta^5$-$C_5Me_4CH_2\overline{C_6H_4}$)Fe(CO)$_2$, 100909-62-4; ($\eta^5$-$C_5Me_4Bz$)Fe-(CO)(^{13}CO)Me, 100909-63-5; (η^5-C_5H_4Bz)Fe(CO)(PPh$_3$)Me, 100909-64-6; (η^5-C_5Me_4Bz)Fe(CO)(PPh$_3$)Me, 100909-65-7; (η^5-$C_5H_4CH_2\overline{C_6H_4}$)Fe(CO)(PPh$_3$), 100909-66-8; ($\eta^5$-$C_5Me_4CH_2$-$\overline{C_6H_4}$)Fe(CO)(PPh$_3$), 100909-67-9.

Supplementary Material Available: Listings of thermal parameters and of structure factor amplitudes for (η^5-$C_5Me_4CH_2\overline{C_6H_4}$)Fe(CO)$_2$ (13 pages). Ordering information is given on any current masthead page.

Structural Characterization of (η^5:η^5-$C_{10}H_6(CH_3)_2$)[(η^5-$C_5H_4CH_3$)MoH]$_2$. An Alternative Configuration for the Dinuclear Structure of Molybdenocene

James W. Egan, Jr., and Jeffrey L. Petersen*

Department of Chemistry, West Virginia University, Morgantown, West Virginia 26506-6045

Received August 19, 1985

An X-ray structure determination of (η^5:η^5-$C_{10}H_6(CH_3)_2$)[(η^5-$C_5H_4CH_3$)MoH]$_2$ has been performed and confirms an alternative configuration which had been previously proposed for the dinuclear structure of molybdenocene. The two (η^5-$C_5H_4CH_3$)MoH units are bridged symmetrically by a π-fulvalene ligand. Each Mo atom achieves a filled valence shell configuration by bonding through a long two-electron Mo–Mo single bond of 3.3623 (5) Å, to a single terminal hydride ligand (δ −9.22), and in an η^5-fashion to a methylcyclopentadienyl ring and to one ring of the fulvalene bridge. The compound crystallizes in a noncentrosymmetric orthorhombic unit cell of *Fdd*2 symmetry with refined lattice parameters of a = 35.781 (7) Å, b = 34.150 (6) Å, c = 6.382 (2) Å, V = 7798 (3) Å^3, Z = 16, and ρ_{calcd} = 1.732 g/cm^3. Full-matrix least-squares refinement (based on F_o^2) of 2463 diffractometry data converged with final discrepancy indices of $R(F_o^2)$ = 0.0252, $R(F_o^2)$ = 0.0369, and $R_w(F_o^2)$ = 0.0624 with σ_1 = 1.608.

Introduction

The stereochemistry and reactivity of molybdenocene represents a continually challenging area of research in early-transition-metal chemistry. Efforts undertaken by Green and his co-workers[1] during the past decade have led to the development of synthetic routes for the preparation of several dimeric forms of molybdenocene. Treatment of [(η^5-C_5H_5)$_2$MoHLi]$_4$ with N_2O in toluene[2a,b] produces two yellow molybdenocene isomers, *cis*- and *trans*-[(μ-η^1:η^5-C_5H_4)$_2$][(η^5-C_5H_5)MoH]$_2$ (**1** and **2**), which are analogous to structurally characterized tungstenocene compounds.[2c] These compounds have been shown independently by Smart,[3] Green,[1c] and their co-workers to undergo a reductive coupling in toluene at 50 °C to yield a green dimer, (η^5:η^5-$C_{10}H_8$)[(η^5-C_5H_5)MoH]$_2$ (**3**). Although the presence of a bridging fulvalene and terminal hydride ligands in **3** has been supported by NMR and infrared data, the molecular structure of **3** remains to be determined. In this paper we wish to report the isolation and structural characterization of a methylcyclopentadienyl analogue, (η^5:η^5-$C_{10}H_6(CH_3)_2$)[(η^5-$C_5H_4CH_3$)MoH]$_2$ (**4**). The results of our X-ray diffraction analysis of **4** have provided an opportunity to investigate the nature of the Mo–Mo and Mo–H interactions.

Experimental Section

General Considerations. All manipulations were performed by using a combination of glovebox and high vacuum line tech-

(1) (a) Berry, M.; Cooper, N. J.; Green, M. L. H.; Simpson, S. J. *J. Chem. Soc., Dalton Trans.* **1980**, 29. (b) Green, M. L. H.; Simpson, S. J. *J. Organomet. Chem.* **1978**, *148*, C27. (c) Cooper, N. J.; Green, M. L. H.; Couldwell, C.; Prout, K. *J. Chem. Soc., Chem. Commun.* **1977**, 145.

(2) (a) Green, M. L. H.; Poveda, M. L.; Bashkin, J.; Prout, K. *J. Chem. Soc., Chem. Commun.* **1982**, 30. (b) Bashkin, J.; Green, M. L. H.; Poveda, M. L.; Prout, K. *J. Chem. Soc. Dalton Trans.* **1982**, 2485. (c) Couldwell, C.; Prout, K. *Acta Crystallogr., Sect. B: Struct. Crystallogr. Cryst. Chem.* **1979**, *B35*, 335.

(3) Smart, J. C.; Curtis, C. J. *Inorg. Chem.* **1978**, *17*, 3290.

0276-7333/86/2305-0906$01.50/0